Int. J. Electrochem. Sci., 12 **(2017)** 3212 – 3220, doi: 10.20964/2017.04.59

International Journal of
ELECTROCHEMICAL
SCIENCE
www.electrochemsci.org

Pre-lithiated Mesocarbon Microbeads Anode and Bifunctional Cathode for High Performance Hybrid Lithium-Ion Capacitors

Jing Li[*], *Jianqiang Guo*[*], *Pengyu Li, Lige Wang, Yeju Huang*

School of Materials Science and Engineering, Southwest University of Science and Technology, Mianyang, Sichuan 621010, China
[*]E-mail: 2775262938@qq.com

Received: 30 December 2016 / *Accepted:* 21 February 2017 / *Published:* 12 March 2017

Lithium-ion capacitor (LIC) is a hybridization of two types of electrochemical energy storage system, rechargeable battery and electrochemical double layer capacitor. Scientific researchers have made broad research on the LIC in the past decades. In this paper, we used pre-lithiated mesocarbon microbeads anode and bifunctional cathode including 75 wt.% capacitor material (activated carbon (AC)) and 25 wt.% battery material (lithium iron phosphate (LFP)) to prepare hybrid lithium-ion capacitors (LIC (AC+LFP)). The results show that the as-prepared LIC (AC+LFP) hybrid lithium-ion capacitors exhibit better cycle stability and higher rate performance, compared with the LIC (AC) hybrid lithium-ion capacitors, which only employs AC as cathode matertials. This improved performance is mainly due to the addition of LFP in the cathode electrode.

Keywords: Hybrid lithium-ion capacitor; Pre-lithiated; AC; MCMB； LFP

1. INTRODUCTION

With the demand for electric vehicles increasing in the past decades, the requirements for energy storage sources that can provide both high power and high energy are extremely urgent [1-5]. In order to satisfy the need for both high power and high energy, many different approaches for developing electrochemical energy storage systems have been proposed. Among these different approaches, the most viable candidate is the hybrid lithium-ion capacitor (LIC), which is the hybridization of rechargeable lithium-ion battery and electrochemical double layer capacitor [6-11].

Several papers published about different types LIC have been mentioned. Amatucci et al. [12] firstly reported the internal serial hybridization system using activated carbon (AC) as cathode and $Li_4Ti_5O_{12}$ anode. Ping et al. [13] prepared the hybrid lithium-ion capacitor (LIC) using pre-lithiated

mesocarbon microbead (pre-lithiated MCMB) as negative electrode and activated carbon (AC) as positive electrode. After that, other carbonaceous materials for the anode materials of LIC, e.g., graphite [14, 15], soft carbon [16], hard carbon [17], graphene nanosheets [18-21] were extensively investigated and even successfully commercialized. From these studies, it can be known that much efforts in researching the anode materials, relatively little attentions have been paid on the cathode materials.

Hence, in this work, we use pre-lithiated mesocarbon microbead (pre-lithiated MCMB) as anode and (AC+ lithium iron phosphate (LFP)) bifunctional electrode as cathode to prepare the hybrid lithium-ion capacitor (LIC (AC+LFP)). Compared with the hybrid lithium-ion capacitor (LIC (AC)) which only employs AC as cathode, the LIC (AC+LFP) exhibits superior electrochemical performances. Especially, the energy density of the LIC (AC+LFP) is up to 30 Wh kg^{-1}, which is two times than the LIC (AC).

2. **EXPERIMENTAL**

2.1 Preparation of cathode electrode

The cathode electrode slurry was prepared by mixing 80 wt.% active material (AC(75%)+LFP(25%) or AC), 10 wt.% conductive carbon black and 10 wt.% polyvinylidene fluoride (PVDF) binder in N-methyl pyrrolidinone (NMP) solvent. The slurry was then coated onto aluminum foil and dried at 60℃ in vacuum for 24 h. The electrode was subsequently punched out a circular disk with an 15 mm diameter.

2.2 Preparation of anode electrode

The anode electrode slurry was prepared by mixing 80 wt.% MCMB, 10 wt.% conductive carbon black and 10 wt.% polyvinylidene fluoride (PVDF) binder in N-methyl pyrrolidinone (NMP) solvent. The mixed slurries were immediately casted onto copper foil, dried in oven at 80℃ for 24 h, and then left at room temperature overnight. The electrode was subsequently punched out a circular disk with an 15 mm diameter.

2.3 Fabrication of cells

Pre-lithiation process of MCMB electrode was carried out by galvanostatic discharging in coin cell (CR2016), which assembled with MCMB working electrode and lithium countering electrode. The current density for pre-lithiation is 6 mA g^{-1}, and the discharge specific capacity is about 384 mAh g^{-1}(based on MCMB mass). The typical voltage profile of pre-lithiation process for MCMB anode is depicted in Fig. 1.

To understand the cathode and anode potentials of LIC, three-electrode LIC was assembled by AC+LFP or AC cathode and pre-lithiated MCMB anode, with lithium metal as the reference electrode.

. The electrolyte was 1.2 mol L^{-1} LiPF6 in 1:1 EC/DEC (ethylene carbonate/diethyl carbonate), and a porous polypropylene microporous sheet was used as the separator. All cells were assembled in an Argon-filled glove box.

2.4 Electrochemical test

The galvanostatic charge-discharge tests were investigated by a LAND CT2001A battery testing system. Three electrode tests were conducted by using Li^+/Li as reference electrode. Cyclic voltammetry measurements and electrochemical impedance spectra (EIS) measurement were carried out on an electrochemistry workstation (CHI660E). The energy and power density were calculated per active materials mass of two electrodes.

3. RESULTS AND DISCUSSION

3.1 Electrochemical performance of MCMB

As shown in Fig.1, it displays the voltage profile of pre-lithiation process for MCMB anode at a current density of 0.05 C. The first intercalation capacity obtained for MCMB is 384 mAh g^{-1}. Besides, it can be seen that the curve show sloping profiles from 1.2 to 0.2 V during the discharge process (lithium intercalation), and relatively flat plateaus below 0.2 V. Moreover, during the cathodic scan (Fig.1 inset) a peak at the potential of about 1.2 V before the intercalation of lithium-ion into MCMB, which indicates that a reductive decomposition of electrolyte occurs and the decomposition products form the solid electrolyte interface (SEI) film on MCMB surface. Thus, we can believe that the irreversible capacity loss is associated with the formation of SEI film [22, 23].

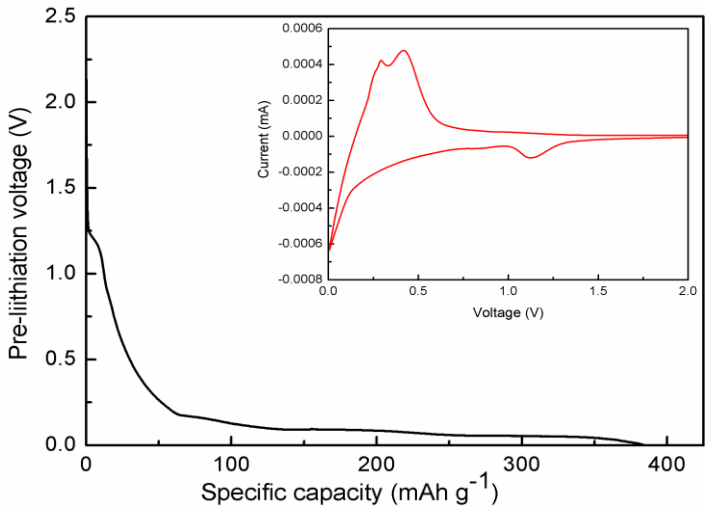

Figure 1. Voltage profile of pre-lithiation process for MCMB anode at a current density of 0.05 C: Inset shows the cyclic voltammograms of Li/MCMB cell at a scan rate of 0.02 mV s^{-1}.

3.2 Electrochemical performance of LIC (AC) and LIC (AC+LFP)

The electrochemical performances of LIC (AC) and LIC (AC+LFP) were investigated by using galvanostatic charge/discharge measurements at the current density of 50 mA g^{-1}. The voltage profiles are shown in Fig.2. The voltage profiles in Fig. 2 (a) are in isosceles triangle shape, which indicates its electric doublelayer capacitor characteristic [24]. The obtained voltage profiles (Fig.2 (a)) of LIC (AC) are nearly linear and symmetric, indicating a perfect capacitive behavior. Compare to the profiles of LIC (AC), the profiles of (Fig.2 (b)) LIC (AC+LFP) show both battery and capacitor characteristic during the charging/discharging process due to the presence of LFP in the cathode. Therefore, the LIC (AC+LFP) hybrid lithium-ion capacitors present excellent cycle stability and high energy density in the following electrochemical performances.

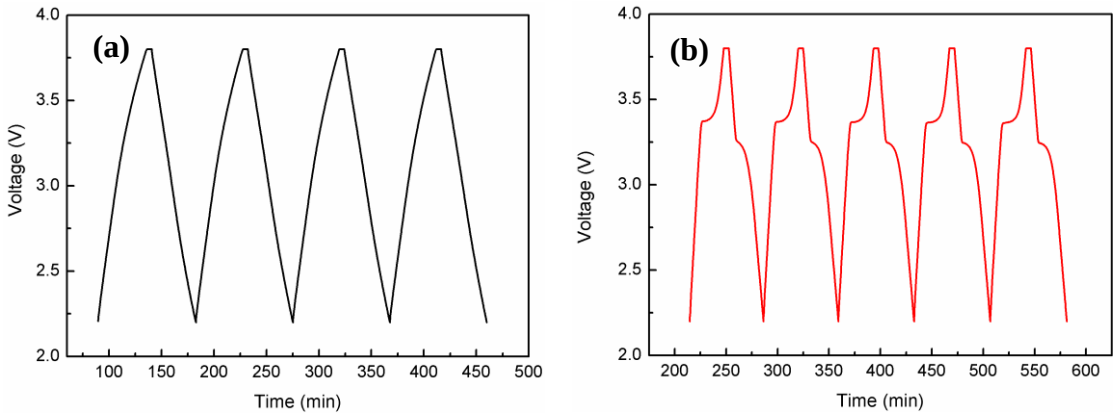

Figure 2. Voltage profiles for (a) LIC (AC); (b) LIC (AC+LFP) lithium-ion hybrid capacitors at the current density of 50 mA g^{-1}.

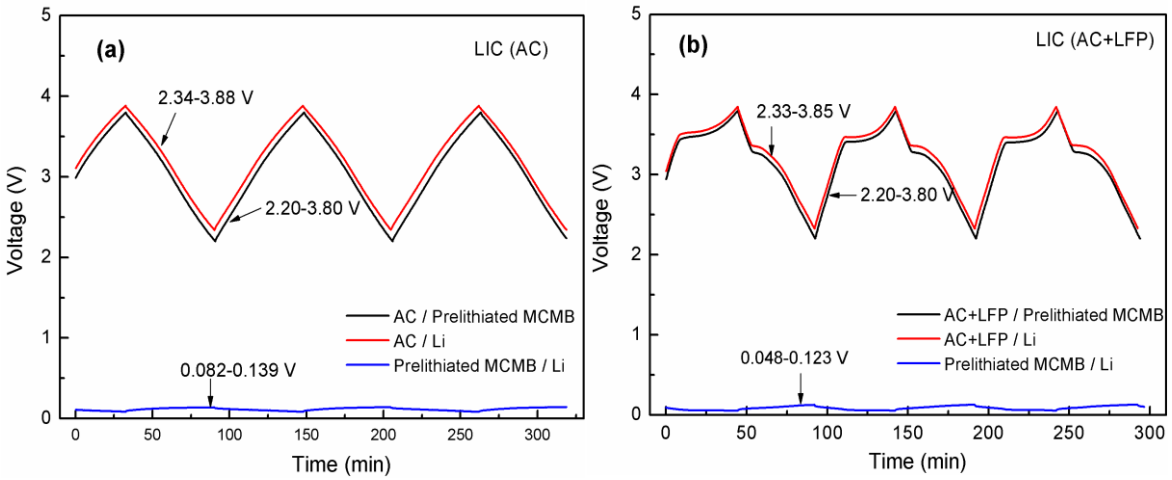

Figure 3. Galvanostatic charge-discharge profiles during the first three cycles for three-electrode full cells in the voltage range of 2.0-4.0 V: (a) LIC (AC); (b) LIC (AC+LFP) hybrid lithium-ion capacitors.

To understand the voltage change of both cathode and anode electrodes, the voltage profiles vs. Li^+/Li reference electrode are shown in Fig. 3a and b. The voltage versus time curves for LIC (AC) are linearly proportional to the charge/discharge time in the voltage range of 2.0-4.0 V. The cathode potential varies from 2.34 to 3.88 V vs. Li+/Li. The anode potential value swings from 0.082 to 0.139, which is minor change. Therefore, the voltage change (2.20-3.80 V) of whole LIC (AC) hybrid lithium-ion capacitor can be approximated as voltage change of cathode electrode. For LIC (AC+LFP) hybrid lithium-ion capacitor, it shows similar voltage change. The only difference is that the whole cell voltage and cathode voltage profiles exhibit battery characteristic [25], which is ascribed to the capacity contribution of LFP in the cathode.

Cyclic voltammetry of LIC (AC) and LIC (AC+LFP) hybrid lithium-ion capacitors was used to test the electrochemical performance of LIC (AC) and LIC (AC+LFP) hybrid lithium-ion capacitors. Fig.4 exhibits the CV curves of LIC (AC) and LIC (AC+LFP) at a scan rate of 0.1 mV s^{-1}. According to CV curve for LIC (AC), it can be seen that no obvious redox peaks are observed in the potential window. Besides, the curve has good symmetry and is close to rectangular, which suggests typical capacitor characteristics and excellent reversibility. For the CV curve of LIC (AC+LFP), it shows same rectangular shape except a reduction peak and oxidation peak. This results also prove that the LFP make capacity contribution in the charging/discharging process, leading to a higher capacity than LIC (AC) hybrid lithium-ion capacitor.

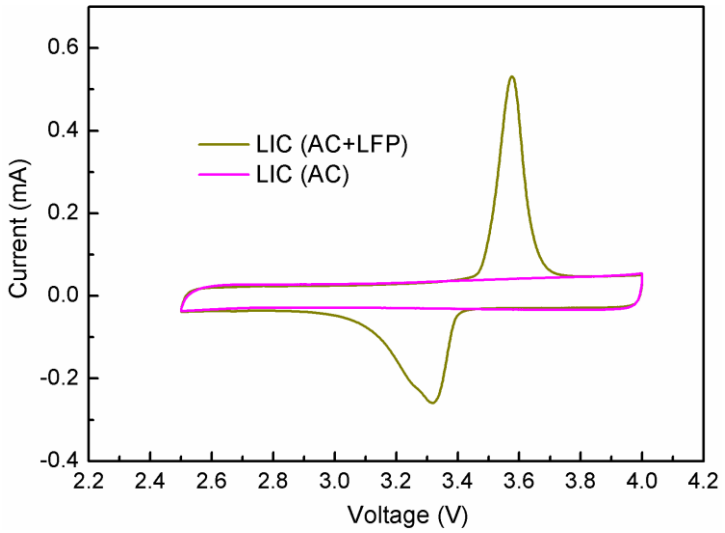

Figure 4. Cyclic voltammogram profiles of LIC (AC) and LIC (AC+LFP) hybrid lithium-ion capacitors at a scan rate of 0.1 mV s^{-1}.

To further understand the superior performance of LIC (AC+LFP) hybrid lithium-ion capacitors, rate performance of LIC (AC) and LIC (AC+LFP) hybrid lithium-ion capacitors were tested at various current density from 50 mA g^{-1} to 1000 mA g^{-1}. Overall, the LIC (AC+LFP) hybrid lithium-ion capacitors exhibit excellent rate performance. It can be seen that the LIC (AC+LFP) hybrid lithium-ion capacitors could endure various current densities even at high current density of 1000

mAg^{-1}. However, as is known to all, the addition of battery material (LFP) in the cathode electrode have a negative effect on the rate performance. Therefore, as shown in Fig.5, the specific capacities of LIC (AC+LFP) fade more serious than LIC (AC) with the increase of current density. However, in terms of capacity contribution, it can be seen that the LIC (AC+LFP) delivers high specific capacities of 51 mAh g^{-1} and 43 mAh g^{-1} at the current density of 200 mA g^{-1} and 500 mA g^{-1}, respectively. Even when the current density was improved to 1000 mA g^{-1}, the specific capacitiy still remain to be 40 mAh g^{-1}. Regarding to the LIC (AC), the specific capacities of LIC (AC) are 37 mAh g^{-1} and 34 mAh g^{-1} at the current density of 200 mA g^{-1} and 500 mA g^{-1}. All in all, although the rate performance is reduced due to the presence of LFP, the specific capacities are greatly improved.

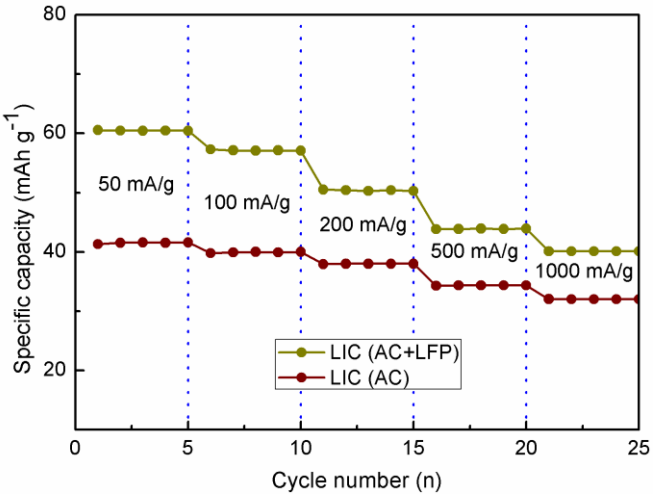

Figure 5. The rate performance of LIC (AC) and LIC (AC+LFP) hybrid lithium-ion capacitors at various current density from 50 mA g^{-1} to 1000 mA g^{-1}.

Fig.6 (a) shows the cycle life of LIC (AC) and LIC (AC+LFP) hybrid lithium-ion capacitors at a voltage range of 2.2-3.8 V. It can be seen that LIC (AC) has a lower capacity retention than LIC (AC+LFP). The capacity retention of LIC (AC+LFP) increases slightly before 100 cycles, and remains constant (nearly 100 %) after 100 cycles. EIS was carried out for the LIC (AC) and LIC (AC+LFP) hybrid lithium-ion capacitors. As shown in Fig.6 (b), all the EIS are composed of semicircles in the high frequency region and a straight line at the low frequency. The semicircle in the high frequency region can be related to the lithium ion migration resistance through the SEI film and the contact resistance of electrolyte/ electrode (R_S) and the charge-transfer resistance (R_{CT}), The low frequency straight line is associated with the diffusion impedance of electrolyte ions as called Warburg impendence [26-28]. The curves of the LIC (AC) and LIC (AC+LFP) are similar with a typical semicircle in the high-medium frequency region and an inclined line at low frequency region. Apparently, the semicircle diameter of LIC (AC+LFP) is much smaller than that of LIC (AC), indicating improved electron conductivity. As a result, the LIC (AC+LFP) hybrid lithium-ion capacitors display superior electrochemical performance than LIC (AC) hybrid lithium-ion capacitors .

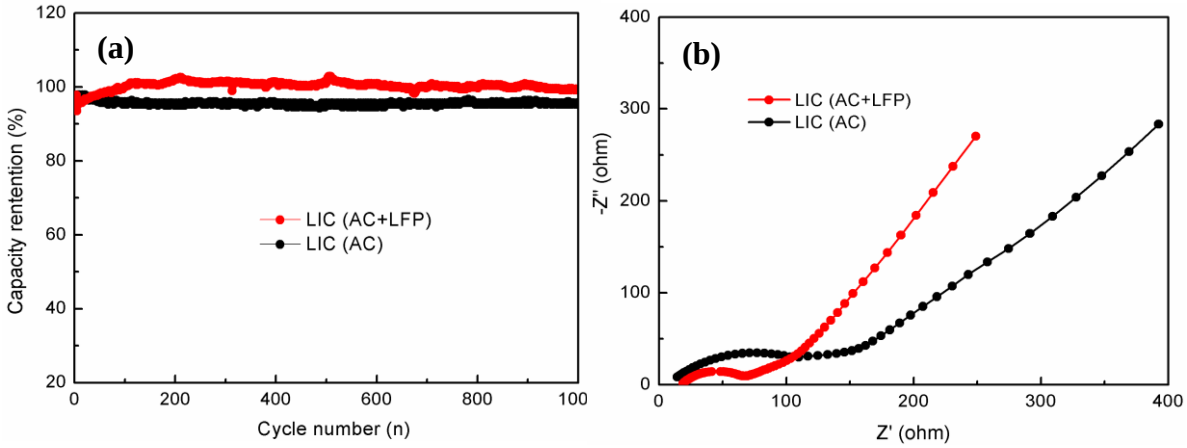

Figure 6. (a) The cycle performance of LIC (AC) and LIC (AC+LFP) hybrid lithium-ion capacitors; (b) EIS curves of LIC (AC) and LIC (AC+LFP) hybrid lithium-ion capacitors.

A new table was made to compare the anode/chatode materials with similar anode/cathode materials that were described in literature for hybrid lithium-ion capacitors. As shown in Table 1, the LIC (AC+LFP) exhibits superior cycle performances than other similar lithium-ion capacitors.

Table 1. Comparison the anode/chatode materials with similar anode/cathode materials.

Materials	Current densities ($mA\ g^{-1}$)	capacity retentions (%) (cycle number)	Reference
LIC (AC+LFP)	60	100 (1000 cycles)	This work
LIC ($Li_4Ti_5O_{12}$)	50	98 (1000)	29
LIC ($LiMn_2O_4$+graphene)	50	91 (500)	30

The energy density and power density for LIC (AC) and LIC (AC+LFP) hybrid lithium-ion capacitors are calculated on the basis of cathode and anode electrode, as shown in Fig. 7. The LIC (AC+LFP) hybrid lithium-ion capacitor demonstrates much higher gravimetric energy density than LIC (AC) hybrid lithium-ion capacitor.

Based on the above results, it can be found that the LIC (AC+LFP) hybrid lithium-ion capacitor presents higher electrochemical performance than LIC (AC) hybrid lithium-ion capacitor. Specifically, the comparisons of electrochemical performance for LIC (AC) and LIC (AC+LFP) at the current density of 50 $mA\ g^{-1}$ are listed in Table 2.

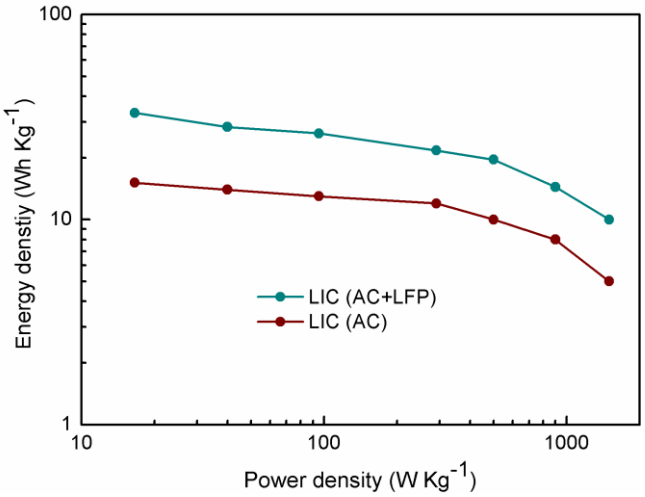

Figure 7. Ragone plots for the LIC (AC) and LIC (AC+LFP) hybrid lithium-ion capacitors on the gravimetric basises.

Table 2. Comparison of electrochemical performance for the LIC (AC) and LIC (AC+LFP) hybrid lithium-ion capacitors at the current density of 50 mA g^{-1}.

Sample	Capacity (mAh g^{-1})	Capacity retentions (%)	Energy density (Wh Kg^{-1})
LIC (AC)	41	98 (1000 cycles)	15
LIC (AC+LFP)	60	100 (1000 cycles)	30

4. CONCLUSIONS

In the present work, the mesocarbon microbeads (MCMB) electrodes were pre-lithiated via galvanostatic discharging in coin cell assembled with MCMB working electrode and lithium countering electrode. After that, the bifunctional electrodes (AC+LFP) were used to fabricate LIC (AC+LFP) hybrid lithium-ion capacitors. The results show that the electrochemical performance of hybrid lithium-ion capacitors can be improved by using bifunctional cathode (AC+LFP) via the addition of LFP in cathode electrode.

ACKNOWLEDGEMENT
This research was supported by the National Natural Science Foundation of China (Grant No. 14Zg1102).

References

1. P. Simon and Y. Gogotsi, *Nat. Mater.*, 7 (2008) 845.

2. H. S. Choi and C. R. Park, *J. Power Sources*, 259 (2014) 1.
3. L. L. Zhang and X. S. Zhao, *Chemical Society Reviews*, 38 (2009) 2520.
4. A. G. Pandolfo and A. F. Hollenkamp, *J. Power Sources*, 157 (2006) 11.
5. E. Frackowiak and F. Béguin, *Carbon*, 39 (2001) 937.
6. J. M. Nan, D. M. Han and X. X. Zuo, *J. Power Sources*, 152 (2005) 278.
7. M. Armand, F. Endres, D. R. MacFarlane, H. Ohno and B. Scrosati, *Nat. Mater*., 8 (2009) 621.
8. P. Sharma and T. S. Bhatti, *Energy Convers Manage*, 50 (2010) 2901.
9. X. Z. Sun, X. Zhang, H. T. Zhang, N. S. Xu, K. Wang and Y. W. Ma, *J. Power Sources*, 270 (2014) 318.
10. J. Y. Liu, M. Lu, J. M. Yang, J. Chen and W. S. Cai, *Electrochim. Acta*, 151 (2015) 312.
11. A. Rudge, J. Davey, I. Raistrick, S. Gottesfeld and J. P. Ferraris, *J. Power Sources*, 47 (1994) 89.
12. G. G. Amatucci, F. Badway, A. Du Pasquier and T. Zheng, *J. Electrochem. Soc.*, 148 (2001) A930.
13. L. N. Ping, J. M. Zheng, Z. Q. Shi and C. Y. Wang, *Acta Phys. Chim. Sin.*, 28 (2012) 1733.
14. M. M. Hantel, T. Kaspar, R. Nesper, A. Wokaun and R. Kotz, *ECS Electrochem. Lett*., 1 (2012) A1.
15. S. R. Sivakkumar, J. Y. Nerkar and A. G. Pandolfo, *Electrochim. Acta*, 55 (2010) 3330.
16. M. Schroeder, M. Winter, S. Passerini and A. Balducci, *J. Power Sources*, 238 (2013) 388.
17. J. H. Kim, J. S. Kim, Y. G. Lim, J. G. Lee and Y. J. Kim, *J. Power Sources*, 196 (2011) 10490.
18. J. Li, X. Zhang, J. Q. Guo, R. F. Peng, R. S. Xie, Y. J. Huang and Y. C. Qi, *J. Alloy. Compd*., 674 (2016) 44.
19. J. J. Ren, L. W. Su, X. Qin, M. Yang, J. P. Wei, Z. Zhou and P. W. Shen, *J. Power Sources*,264 (2014) 108.
20. N. L. Chen, Y. P. Ren, P. P. Kong, L. Tan, H. X. Feng and Y. C. Luo, *App. Sur. Sci*., 392 (2017) 71.
21. Y. Wang, Z. Q. Shi, Y. Huang, Y. F. Ma, C. Y. Wang, M. M Chen and Y. S.Chen, *J. Phys. Chem. C*, 113 (2009) 13103.
22. J. Shim and K. A. Striebel, *J. Power Sources*, 130 (2004) 247.
23. J. Zhang, Z. Q. Shi and C. Y. Wang, *Electrochim. Acta*, 125 (2014) 22.
24. X. L. Yu, J. J. Deng, C. Z. Zhan, R. T. Lv, Z. H. Huang and F. Y. Kang, *Electrochim. Acta*, 228 (2017) 76.
25. X. Z. Sun, X. Zhang, H. T. Zhang, N. S. Xu, K. Wang and Y. W. Ma, *J. Power Sources*, 270 (2014) 318.
26. J. Zhang, X. F. Liu, J. Wang, J. L. Shi and Z. Q. Shi, *Electrochim. Acta*,187 (2016) 134.
27. H. P. Du, H. Yang, C. S. Huang, J. J. He, H. B. Liu and Y. L. Liu, Nano Energy, 22 (2016) 615.
28. C. L. Hsieh, D. S. Tsai, W. W. Chiang Y. H. Liu, *Electrochim. Acta*, 209 (2016) 332.
29. T. Rauhala, J. Leis, T. Kallio and K. Vuorilehto, *J. Power Sources*, 331 (2016) 156.
30. J. Li, X. Zhang, R. F. Peng, Y. J. Huang, L. Guo and Y. C. Qi, *Rsc Adv*., 6 (2016) 54866.